

*Electronic Supporting Information*

**Selective Production of Formate over CuO Electrocatalyst by  
Electrochemical and Photoelectrochemical Biomass  
Valorisation**

Ping-Chang Chuang<sup>a</sup> and Yi-Hsuan Lai<sup>a\*</sup>

<sup>a</sup> Department of Materials Science and Engineering, National Cheng Kung University, No.1,  
University Road, Tainan City 701, Taiwan.

\* Corresponding author: yhlai@gs.ncku.edu.tw

**Contents**

Supporting Tables S1- S4	page S2-S4
Supporting Figures S1–S14	page S5-S11
References	page S12

Table S1. Selected reported literature on the electrochemical valorisation of glucose.

Catalyst	Electrolyte	Potential / V vs RHE	Product	FE / %	Production rate ( $\mu\text{mol cm}^{-2} \text{h}^{-1}$ )	TOF / $\text{h}^{-1}$	Ref
NiFeO <sub>x</sub> -Ni	0.01 M glucose / 1 M KOH	1.30	glucaric acid, gluconic acid	87 (gluconic acid plus glucaric acid)	43.0 (gluconic acid) 416.50 (glucaric acid)	108.0 (gluconic acid plus glucaric acid)	1
Pd <sub>3</sub> Au <sub>7</sub> /C	0.1 M glucose / 0.1 M NaOH	0.40 (vs counter electrode)	gluconate, xylonate, threonate, CO <sub>2</sub>	63.3 (Gluconate)	11.6 (Gluconate)	4.0 (Gluconate)	2
Au/C	0.02 M glucose / 0.1 M NaOH	0.80	gluconate	100 (Gluconate)	N/A	N/A	3
Cu foil	0.1 M glucose / 1 M NaOH	1.46	lactic acid, formic acid	N/A	N/A	N/A	4
Cu	0.04 M glucose / 0.1 M NaOH	1.80	formate, glucaric acid, gluconic acid	N/A	N/A	N/A	5
Pt	0.04 M glucose / 0.1 M NaOH	1.10	formate, glucaric acid, gluconic acid	N/A	N/A	N/A	5
Au	0.04 M glucose / 0.1 M NaOH	0.55	formate, gluconic acid	N/A	N/A	N/A	5
CuBi <sub>2</sub> O <sub>4</sub>	9.8 mM glucose / 0.1 M NaOH	1.64	formate, gluconate	93.00 ± 4.06 (formate)	35.49 ± 6.98	N/A	6
<i>m</i> -CuO	0.02 M glucose / 0.1 M NaOH	1.50	formate	94.1 ± 1.5 (formate)	154.73 ± 10.53	240.2 ± 16.3	This work

**Table S2.** Summary of the generated charge density, formate production rate, and the corresponding FE from 1 h CPE measurements at the various potential in 0.1 M NaOH containing 20 mM glucose.

E / V vs. RHE	Charge density / C cm <sup>-2</sup>	Rate <sub>formate</sub> <sup>a</sup> / μmol cm <sup>-2</sup> h <sup>-1</sup>	FE <sub>Formate</sub> <sup>a</sup> / %	Rate <sub>formate</sub> <sup>b</sup> / μmol cm <sup>-2</sup> h <sup>-1</sup>
1.3	0.46 ± 0.09	2.00 ± 0.49	82.7 ± 4.1	2.39 ± 0.46
1.4	6.41 ± 0.54	30.60 ± 2.02	92.3 ± 2.0	31.17 ± 2.03
1.5	31.70 ± 1.64	154.73 ± 10.53	94.1 ± 1.5	157.32 ± 10.35
1.6	36.80 ± 1.52	175.62 ± 5.97	92.1 ± 0.7	176.91 ± 5.74

<sup>a</sup>Calculated from the amount of formate generated only by electrolysis. <sup>b</sup>Calculated from the total amount of formate, i.e., by electrolysis and self-degradation of glucose in an alkaline solution.

**Table S3.** Summary of the generated charge, FE<sub>Formate</sub>, and the corresponding FE<sub>Formate</sub> from 1 h CPE measurements at 1.5 V vs. RHE catalysing by different catalysts in 0.1 M NaOH containing 20 mM glucose

Electrocatalyst	Charge density / C cm <sup>-2</sup>	R <sub>formate</sub> / μmol cm <sup>-2</sup> h <sup>-1</sup>	FE <sub>Formate</sub> / %
<i>m</i> -CuO	31.70 ± 1.64	154.73 ± 10.53	94.1 ± 1.5
Cu foil	17.54	76.03	83.6
Pre-oxidized Cu foil	28.50	121.09	82.0

**Table S4.** Summary of the generated charge density, R<sub>Formate</sub>, and the corresponding FE<sub>Formate</sub> from 2.5 h CPE measurements at 1.5 V vs. RHE catalysing by *m*-CuO in NaOH containing different substrates (pH 13).

Substrate	Charge density / C cm <sup>-2</sup>	R <sub>formate</sub> / μmol cm <sup>-2</sup> h <sup>-1</sup>	FE <sub>Formate</sub> / %
α-cellulose	0.41 ± 0.12	0.25 ± 0.04	29.7 ± 4.2
Tissue paper	0.53 ± 0.03	0.37 ± 0.01	34.1 ± 3.3
Rice straw	0.78 ± 0.02	0.67 ± 0.16	41.4 ± 9.7

**Table S5.** Selected reported literature of PEC reforming of organic compounds to formate.

Photoelectrode	Cocatalyst	Substrate	Supporting Electrolyte	FE <sub>formate</sub> / %	Ref
W:BiVO <sub>4</sub>	NiO <sub>x</sub> (OH) <sub>y</sub>	Glycerol	0.5 M Na <sub>2</sub> SO <sub>4</sub>	44.8 (1.2 V vs. RHE)	7
			0.5 M KBi (pH 9.2)	31.9 (1.2 V vs. RHE)	
TiO <sub>2</sub>	nanoNi-P <sub>op</sub> (CV)	Ethylene glycol	1 M KOH	57.2 ± 3.1 (0.5 V vs. RHE)	8
TiO <sub>2</sub>	nanoNi-P <sub>op</sub> (CV)	Polyethylene terephthalate	1 M KOH	57.1 ± 1.7 (0.46 V vs. RHE)	8
BiVO <sub>4</sub>	nanoFe:Ni-Bi	Methanol	0.1M borate buffer (pH 9.4)	94.6 ± 12.3 (0.55 V vs. RHE)	9
Fe <sub>2</sub> O <sub>3</sub>	NiBi <sub>(PED)</sub>	Methanol	0.1 M NaOH	77.5 (1.48 V vs. RHE)	10
BiVO <sub>4</sub>	N/A	Glycerol	0.1 M Na <sub>2</sub> B <sub>4</sub> O <sub>7</sub>	N/A	11
Ta <sub>3</sub> N <sub>5</sub>	CoNiFe-LDH	Glycerol	1 M NaOH	60 (1.23 V vs. RHE)	12
Fe <sub>2</sub> O <sub>3</sub>	N/A	Glycerol	0.1 M KOH	N/A	13
Fe <sub>2</sub> O <sub>3</sub>	N/A	Glucose	0.1 M NaOH	60.8 ± 1.5 (1.0 V vs. RHE)	This work
Fe <sub>2</sub> O <sub>3</sub>	<i>m</i> -CuO	Glucose	0.1 M NaOH	97.3 ± 2.8 (1.0 V vs. RHE)	This work

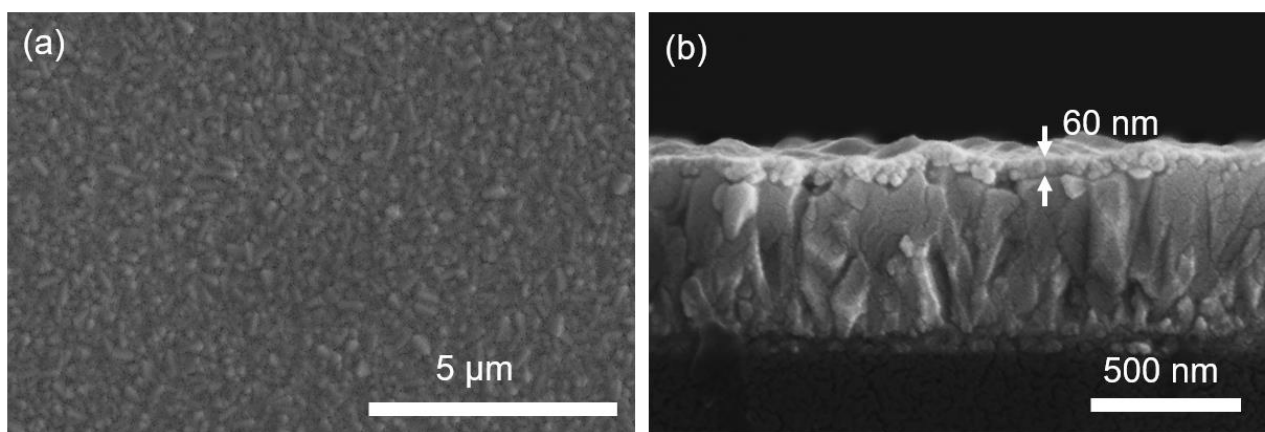


Fig. S1. SEM (a) planar and (b) side view images of *m*-CuO.

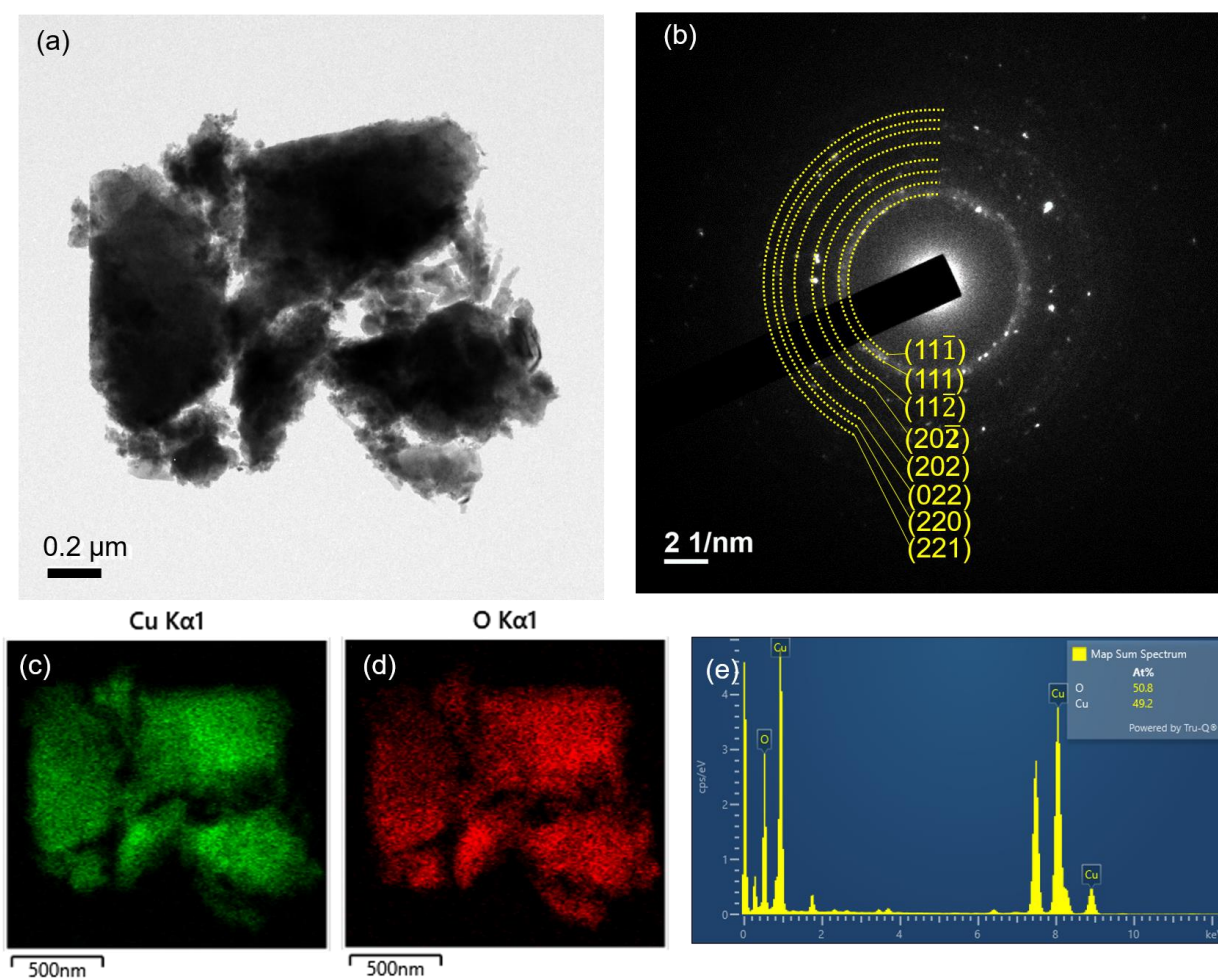


Fig. S2. (a) TEM image, (b) SAED pattern, (c, d) elemental mapping images and (e) EDS spectrum of *m*-CuO.

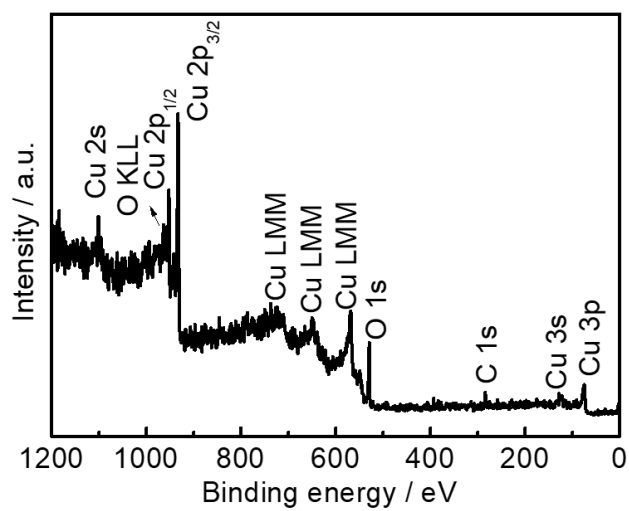


Fig. S3. XPS survey spectrum of *m*-CuO.

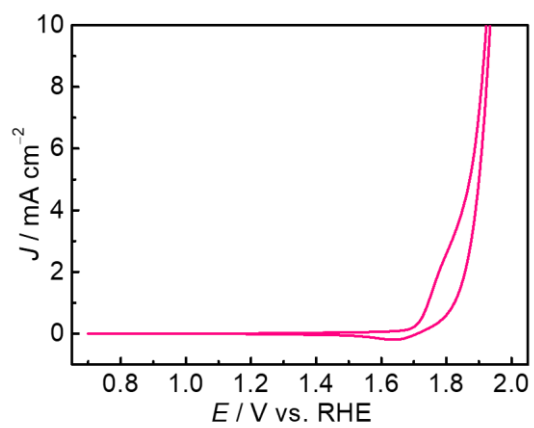


Fig. S4. The CV of *m*-CuO recording at a scan rate of  $50 \text{ mV s}^{-1}$  in the deaerated NaOH solution (0.1 M).

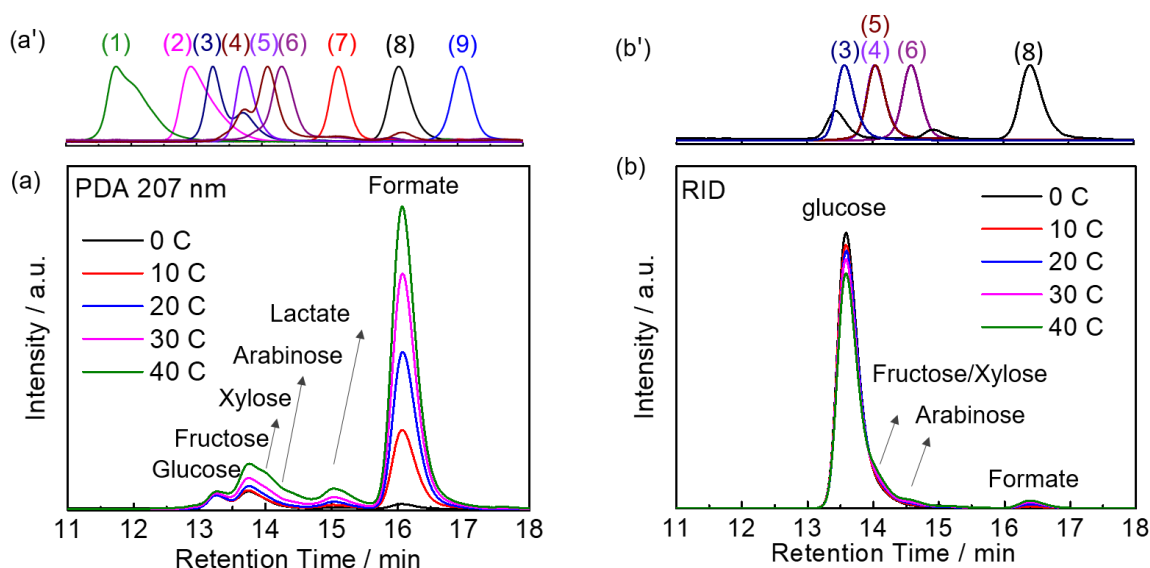


Fig. S5. HPLC chromatograms obtained from (a', a) photodiode array (PDA) and (b', b) refractive index detectors (RID) of (a', b') various standards with normalised intensity and (a, b) the products from the electrochemical oxidation of glucose using *m*-CuO as electrocatalyst at 1.5 V vs. RHE in 0.1 M NaOH containing 20 mM glucose with different amounts of charged passed. Peak 1: glucaric acid, peak 2: gluconic acid, peak 3: glucose, peak 4: fructose, peak 5: xylose, peak 6: arabinose, peak 7: lactate, peak 8: formate, and peak 9: acetate.

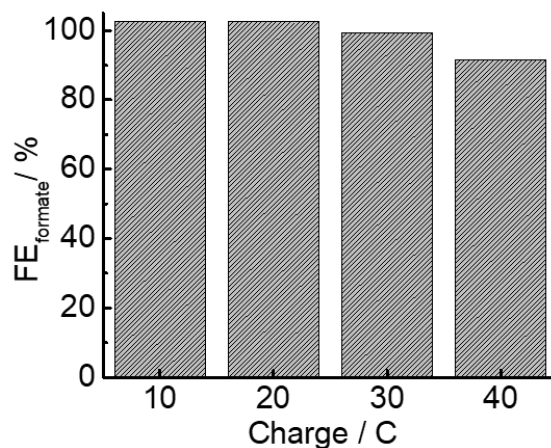


Fig. S6. The FE<sub>formate</sub> as a function of charge passed of *m*-CuO at 1.5 V vs. RHE in deaerated NaOH solution (0.1 M) containing 20 mM glucose. .

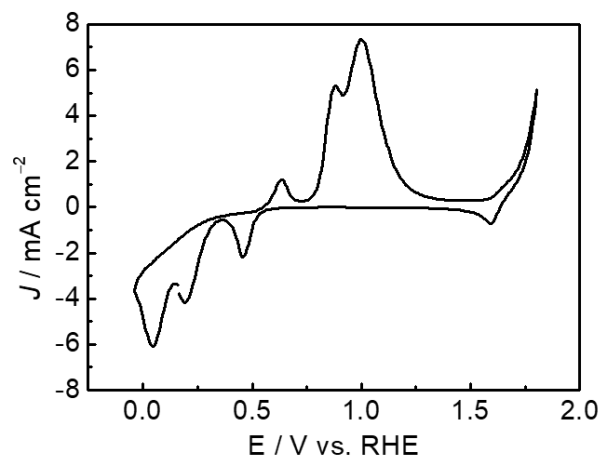


Fig. S7. The cyclic voltammetry scan of Cu foil in 0.1 M NaOH.

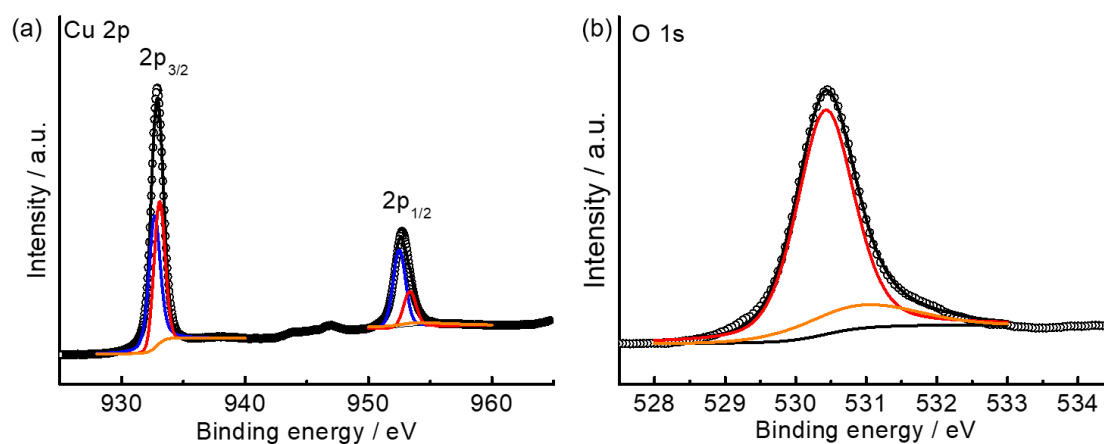


Fig. S8. XPS core-level spectra of the (a) Cu 2p and (b) O 1s region of the pre-oxidised Cu foil. The Cu  $2p_{3/2}$  signals centred at 932.7 eV, 933.1 eV and 934.6 eV are corresponding to the characteristic Cu  $2p_{3/2}$  signals of Cu, CuO and Cu(OH)<sub>2</sub>, respectively.<sup>14</sup> On the other hand, in the O 1s region, the signals centred at 530.4 eV and 530.9 eV are corresponding to the characteristic O 1s signals of CuO and Cu(OH)<sub>2</sub>, respectively.<sup>15</sup>



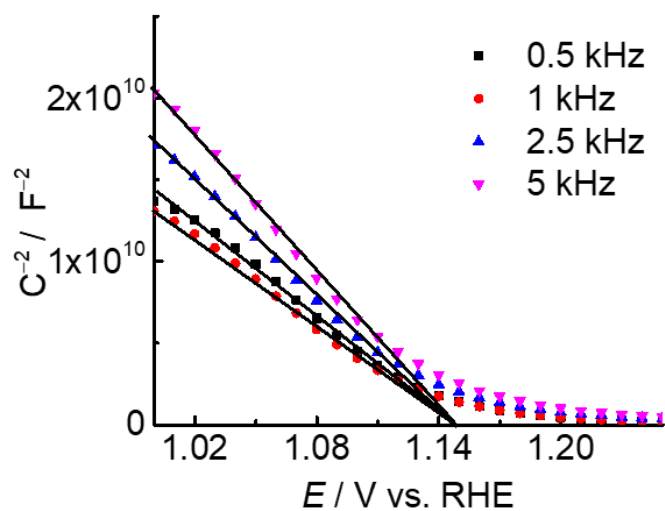


Fig. S9. The Mott-schottky plot of *m*-CuO. The analyses were performed in 0.1 M NaOH at four frequencies and the results suggest the flat band edge of *m*-CuO is approximate 1.15 V vs. RHE.

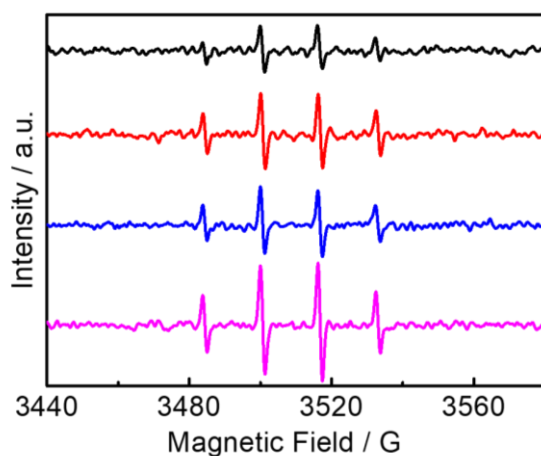


Fig. S10. EPR spectra of *m*-CuO in 1 M NaOH solution before electrolysis (black line) and after 10 min electrolysis at OCP (red line), 1.2 V (blue line) and 1.5 V (pink line) vs. RHE in 1 M NaOH solution.

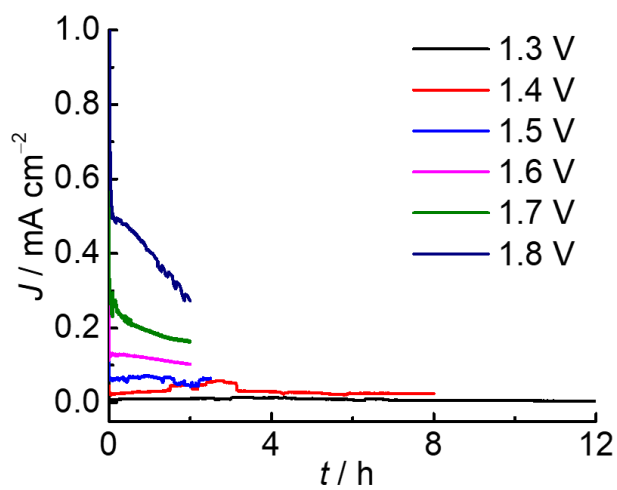


Fig.S11. CPE measurements of *m*-CuO at various potentials (vs. RHE). A NaOH solution containing cellulose (pH 13) was used as the electrolyte.

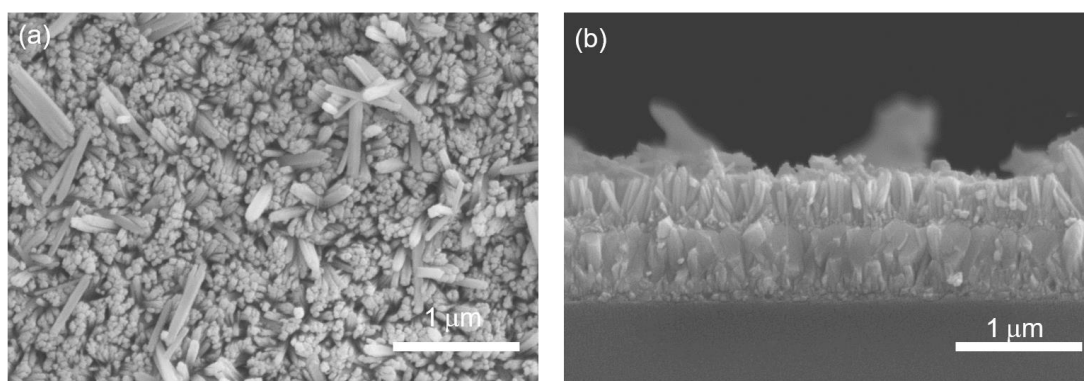


Fig. S12. The SEM images of (a) planar view and (b) side view of FeOOH.

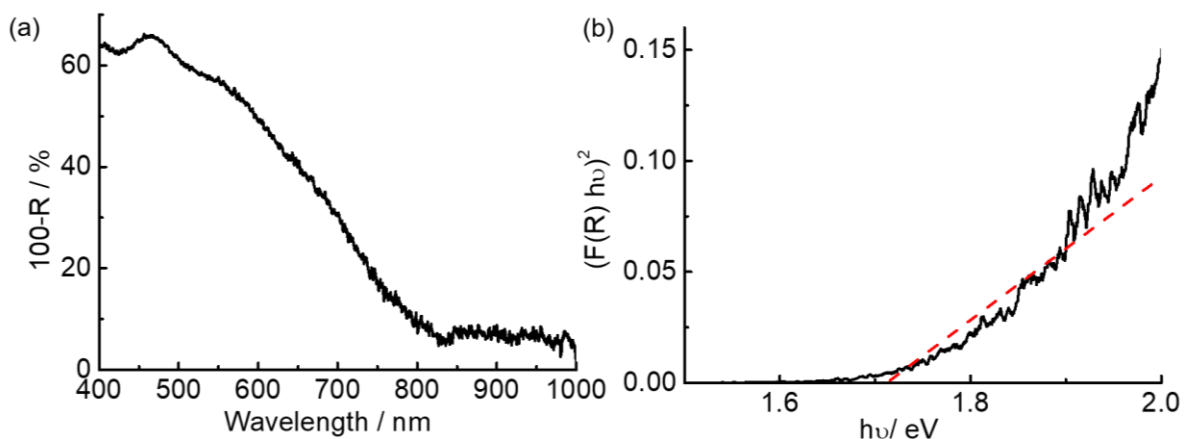


Fig. S13. The (a) UV-vis spectrum and (b) corresponding Tauc plot of *m*-CuO.

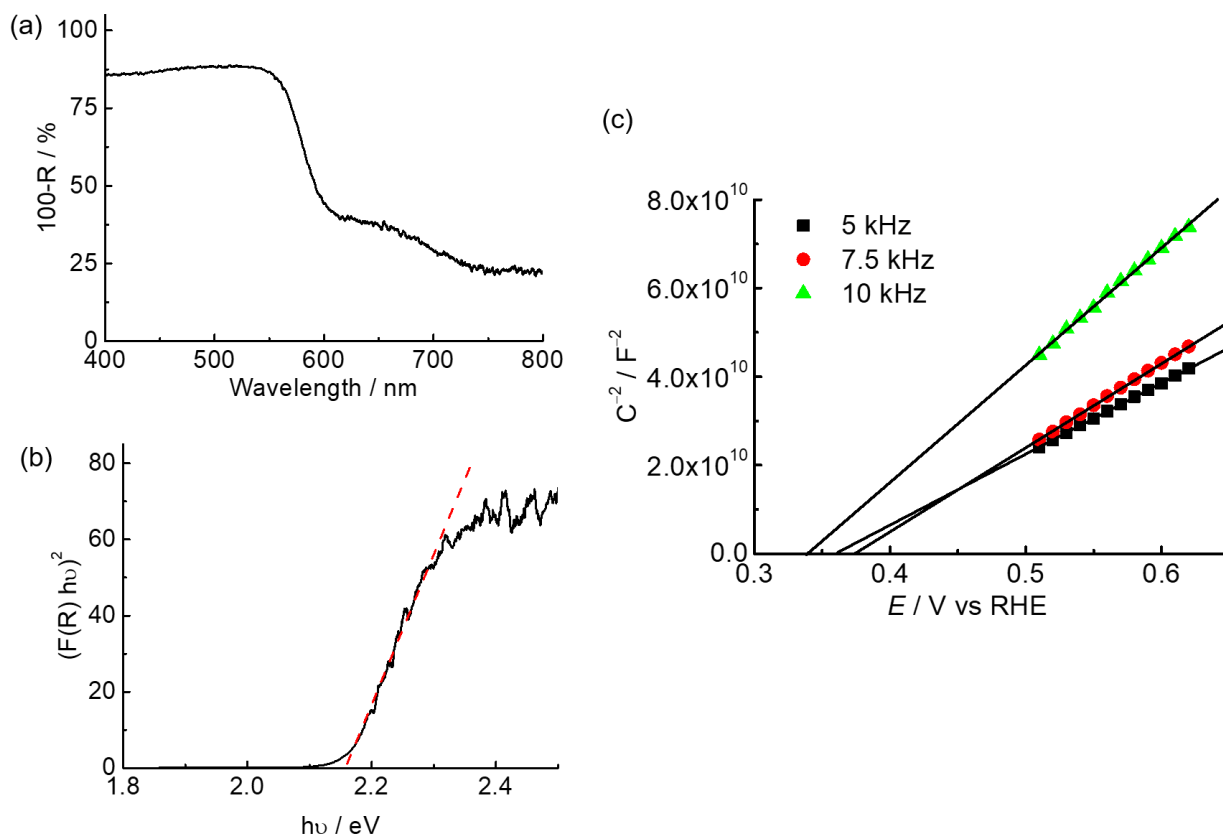


Fig. S14. (a) The UV-vis spectrum, (b) corresponding Tauc plot, and (c) Mott-Schottky analyses plot of nanoFe<sub>2</sub>O<sub>3</sub>. Mott-Schottky analyses were performed in 0.1 M NaOH at frequencies of 5 kHz, 7.5 kHz and 10 kHz.

## Reference

1. W.-J. Liu, Z. Xu, D. Zhao, X.-Q. Pan, H.-C. Li, X. Hu, Z.-Y. Fan, W.-K. Wang, G.-H. Zhao, S. Jin, G. W. Huber and H.-Q. Yu, *Nat. Commun.*, 2020, **11**, 265.
2. T. Rafaïdeen, S. Baranton and C. Coutanceau, *Appl. Catal. B*, 2019, **243**, 641-656.
3. Y. Holade, K. Servat, T. W. Napporn, C. Morais, J. M. Berjeaud and K. B. Kokoh, *ChemSusChem*, 2016, **9**, 252-263.
4. L. Ostervold, S. I. Perez Bakovic, J. Hestekin and L. F. Greenlee, *RSC Adv.*, 2021, **11**, 31208-31218.
5. G. Moggia, T. Kenis, N. Daems and T. Breugelmans, *ChemElectroChem*, 2019, **7**, 86-95.
6. C.-Y. Lin, S.-Y. Lin, M.-C. Tsai and C.-H. Wu, *Sustain. Energy Fuels*, 2020, **4**, 625-632.
7. Y.-H. Wu, D. A. Kuznetsov, N. C. Pflug, A. Fedorov and C. R. Müller, *J. Mater. Chem. A* 2021, **9**, 6252-6260.
8. C.-Y. Lin, S.-C. Huang, Y.-G. Lin, L.-C. Hsu and C.-T. Yi, *Appl. Catal. B*, 2021, **296**, 120351.
9. S.-C. Huang, C.-C. Cheng, Y.-H. Lai and C.-Y. Lin, *Chem. Eng. J.*, 2020, **395**, 125176.
10. C. -Y. Lin, Y. -C. Chueh and C. H. Wu, *Chem Commun*, 2017, **53**, 7345-7348.
11. L.-W. Huang, T.-G. Vo and C.-Y. Chiang, *Electrochim. Acta* 2019, **322**, 134725.
12. Q. Wang, X. Ma, P. Wu, B. Li, L. Zhang and J. Shi, *Nano Energy*, 2021, **89**, 106326.
13. N. Perini, C. Hessel, J. L. Bott-Neto, C. T. G. V. M. T. Pires, P. S. Fernandez and E. Sitta, *J. Solid State Electrochem.*, 2021, **25**, 1101-1110.
14. M. C. Biesinger, *Surf. Interface Anal.*, 2017, **49**, 1325-1334.
15. Z. Zhai, Y. You, L. Ma, D. Jiang, F. Li, H. Yuan, M. Zheng and W. Shen, *Nanoscale Res. Lett.*, 2019, **14**, 167.